Modulation of earth surface air warming by long-term variations of global radiation in Central Europe

Jürg Thudium[1] and Carine Chelala[1]

[1]Affiliation not available

April 23, 2023

Long-term variations of global radiation in Central Europe 1950-2020 and their influence on terrestrial surface air warming

Short title:

Long-term variations of global radiation

Keywords: climate change, surface air temperature, global radiation, global dimming, global brightening, sunshine duration

Authors:

Jürg Thudium[1], Carine Chélala[2]

Affiliations:

[1]Oekoscience AG, Chur, Switzerland. Thudium@oekoscience.ch

[2]Oekoscience AG, Innsbruck, Austria. Chelala@oekoscience.ch

***Corresponding author:**

Jürg Thudium, Oekoscience AG, Postfach 452, CH-7001 Chur.

Thudium@oekoscience.ch

Funding

This work was supported by the environmental authority of the canton of Grisons, Switzerland, for non-personnel costs.

Abstract

Increasing air pollution by aerosols led to a continuous weakening of global radiation at the earth's surface (global dimming) in Europe from about 1950-1980, but during the subsequent improvement of air quality, an increase occurred again (global brightening). Global brightening, which has continued until at least 2020 (end of the study period), has more than compensated for global dimming. In this study the variation of global radiation from 1950-2020 and its cause was investigated based on measurements of sunshine duration, global radiation and temperature from six measuring stations from the national weather services in Austria, Switzerland and Germany.

The phases of global dimming and brightening are mainly caused by increasing and decreasing opacity of the atmosphere by aerosols, which is shown in the distribution of direct solar radiation at Potsdam at different states of cloudiness. From 1982-2020, direct solar radiation increased by about one-third in both the summer and winter months. This increase is at least twice as large as the decrease during the dimming phase, except for the case of nearly overcast sky.

A quantitative estimation of the influence of the fluctuating global radiation on surface air temperature was carried out with the help of a multiple linear regression model based on monthly values from the period 1950-2020, i.e. including the phase of global dimming and global brightening. The applicability of this approach was ensured by a set of five statistical standard tests.

The overall temperature increase from 1950-2020 is dominated by the temporally continuous temperature increase (global warming). However, a fraction of the increase (+0.3 °C resp. +0.5 °C for the entire year resp. summer half-year) is attributed to the increase of global radiation.

With regard to the brightening period in the last four decades (ca. 1980-2020), the fraction of the increase of global radiation within the total temperature increase is substantial: about one third for the entire year (ca. +0.6 °C), even half for the summer half-year (ca. +1.1 °C). The model results are reasonable in view of the comparison with the temperature measurements at the six stations.

Abbreviations

AOD, aerosol optical depth; GHG, Greenhouse gases; GR, Global radiation; DSR, direct solar radiation; SSD, Sunshine duration; TMIN, mean annual minimum temperature; TMAX, mean annual maximum temperature; DWD, Deutscher Wetterdienst; ZAMG, Zentralanstalt für Meteorologie und Geodynamik (Austria).

1. Introduction

Measurements of sunshine duration (SSD) and global radiation (GR) from different regions of the world show a decrease from about 1950 to 1980, followed by an increasing trend (OHMURA, 2006). Several studies investigated this 'global dimming' (OHMURA and LANG, 1989; STANHILL and COHEN, 2001; LIEPERT, 2002) and subsequent 'brightening' (WILD et al., 2005). It cannot be explained by variations in extraterrestrial solar irradiance (FOUKAL et al., 2006).

Global dimming and brightening have subsequently been linked to changes in atmospheric radiative transmittance due to increases and subsequent decreases in anthropogenic aerosol concentrations (NORRIS and WILD, 2007). This was confirmed by RUCKSTUHL et al. (2008) with aerosol optical depth (AOD) measurements from many radiation sites in Northern Germany and Switzerland. The measurements confirmed solar brightening and showed that the direct aerosol effect had an approximately five times larger impact on climate forcing than the indirect aerosol and other cloud effects.

Already 30 years ago, sulfates were identified as the main aerosol influence on the radiation budget (e.g. CHARLSON 1992; KIEHL AND BRIEGLEB 1993). In Austria, emissions of sulfur dioxide have been reduced by 85% from 1990 to 2019 (Federal Environmental Agency of Austria, 2021). In Switzerland, sulfate in the atmosphere has decreased by 80% from 1988 to 2019 (FOEN, 2020); such strong declines are likely typical for most of Europe. Globally, there are major differences in sulfate development. Europe had the largest reductions in sulfur emissions in the first part of the period while the highest reduction in North America and East Asia came later. The uncertainties in both the emissions and the representativity of the observations are larger in Asia. However, emissions from East Asia clearly increased from 2000 to

2005 followed by a decrease, while in India a steady increase over the whole period has been observed and modelled (AAS et al., 2019).

The variations of global radiation over the last 70 years might have impacted the hydrological cycle, through a modulation of the energy available for evapotranspiration. BOÉ (2016) found large inconsistencies in climate models in this regard, mainly related to two properties of the models: the magnitude of the impact of anthropogenic aerosols on solar radiation and whether evapotranspiration is predominantly water or energy limited.

WILD et al. (2021) investigated global dimming and brightening using daily data on global radiation at Potsdam, Germany, over the 71-year period 1947–2017. Strong dimming and brightening tendencies in atmospheric transmission could also be found under clear-sky conditions, which means independent of cloudiness, causing variations in surface solar radiation of about 10 W/m². Variations in atmospheric opacity also in cloud-free atmospheres were therefore identified by the authors as the main contributors to dimming and brightening in Central Europe. They indicated that aerosol pollutants are the likely major drivers for this effect.

SCHERRER and BEGERT (2019) could explain the evolution of mean annual minimum temperature (TMIN) by global forcing and the modifying effects of the large-scale atmospheric flow alone. However they found that local sunshine duration (SSD) information is crucial to explain major features of the mean annual maximum temperature (TMAX) series and the differences between TMIN and TMAX since about 1950. SSD showed no clear trend until 1950, a decline from the period 1950-1980 and an increase since 1980 resembling the global dimming and brightening signal. TMAX was strongly influenced by SSD and its evolution could be well reconstructed with local TMIN and SSD.

KUHN and OLEFS (2020) considered global brightening in the context of elevation dependent warming. The resulting effects do not seem so clear: on the one hand, global brightening is expected to have more impact at low altitudes because the optical thickness of the aerosol has decreased more there since the 1980s than at higher altitudes, but on the other hand, the warming in the Alps is larger than in the surrounding lowlands. Other altitude-dependent processes also seem to play an important role.

In summary, there is substantial evidence that increased air pollution since the 1950s and successful air pollution abatement since the 1980s are primarily responsible for global dimming and brightening.

In this study, a quantitative estimation of the influence of varying global radiation on surface air temperature was carried out with the help of a multiple linear regression model based on monthly values from the period 1950-2020, i.e. during the global dimming period and the global brightening period. Sunshine duration, global radiation and temperature data from six stations in Switzerland, Austria and Germany were analyzed.

2. Measurements

2.1 Measuring Stations

Monthly data on global radiation, temperature and sunshine duration from three national meteorological services (MeteoSchweiz for Switzerland, ZAMG for Austria and DWD for Germany) from 1950 to 2020 were used in this study. In total, results from four stations from Switzerland, one station from Austria and one from Germany were analyzed. Global radiation measurement series at these stations are amongst the longest in existence. Table 1 shows the coordinates and measurement durations of the stations, and their geographical location is indicated in Figure 1.

2.2 Viewing meteorological long time data series

For a long time series of meteorological date, traceability is a special challenge. The national meteorological services make earnest efforts to homogenize these data. Within the framework of this study, no further adaptations of the data delivered from the national meteorological services were made with one small exception (cf. below).

The monthly data of the four **Swiss** stations (Basel, Bern, Genève, Zürich) with regard to global radiation, temperature and sunshine duration were homogenized by MeteoSchweiz

(BEGERT ET AL 2003; MOESCH AND ZELENKA 2004; DÜRR ET AL. 2016; SCHERER AND BEGERT 2019).

The monthly data of the **German** station (Potsdam) with regard to global radiation, temperature and sunshine duration were homogenized by DWD. In particular, the global radiation measurements have been subjected to careful homogenization (as reported by WILD et al, 2021) and regular calibrations have taken place since 1947.

For the **Austrian** station (Wien), the database of HISTALP (Historical Instrumental Climatological Surface Time Series of The Greater Alpine Region, a project from ZAMG) for homogenized monthly values of temperature and sunshine was analyzed (AUER et al, 2007; BÖHM et al, 2009). Monthly data from global radiation were taken from ZAMG. Since systematic homogenization of the global radiation measurement series from ZAMG could not be conducted so far, only data from the station at Wien (Hohe Warte) were used. “Regular calibration of the radiation measuring instrument reduces the uncertainty due to changing instrument sensitivity to a minimum and ensures the traceability of the measurements to the WRR (World Radiometric Reference) in Davos” (TEUBNER, ZAMG, private communication 2021). In April 1991, a new device was installed at the station in Vienna (an electric Starpyranograph was replaced by a Starpyranometer Schenk 8101); an obvious shift due to this equipment replacement was corrected by raising the readings before April 1991 by 3%. This was the only change in measurement data made in this study.

3. Global dimming and brightening: long-term observational records of temperature, global radiation and sunshine duration

The typical long-term observational records of temperature, global radiation (GR) and sunshine duration (SSD) are illustrated with two examples: Basel and Potsdam (Figure 2). A gliding average of five years is presented to bring the long-term trend into focus.

The parallel nature of variations in sunshine duration, global radiation and temperature is obvious, whereby the temperature curve is underpinned by a continuous increase. From about 1950-1980 a decrease in sunshine duration (and global radiation, cf. Potsdam) and a stabilization of temperature can be seen, followed from about 1980-2020 by an increase of SSD and GR together with an increased temperature rise. Dimming and brightening of SSD are found at all stations, and of GR at Potsdam; the measurement of global radiation does not go back as far as sunshine duration and temperature (cf. table 1).

Viewed across all six stations the increase of measured GR from the period 1982-2020 was 14.4 ± 4.8 W/m^2 (average ± standard deviation), corresponding to about 11% of global radiation at the beginning of the 1980s. The increase of SSD was 28.9 ± 8.3 h/month corresponding to about 21% of SSD at the beginning of the 1980s. During the dimming period 1950-1981, the decrease of SSD was -19.6 ± 4.8 h/month corresponding to about -13% of SSD at the beginning of the 1950s. For Potsdam, the increase of GR from 1982-2020 (+15%) was about the double of the decrease 1950-1981 (-7%). For all measured SSD and GR, the effect of global brightening exceeds that of global dimming distinctly. As pointed out by RUCKSTUHL et al. (2008) and WILD et al. (2021), and as can be seen from measured data at Potsdam, this development of GR depends mainly on atmospheric opacity.

In the next section, the causes of the change in global radiation will be discussed in more detail.

4. On the causes of the long-term variations of global radiation

The statements of this chapter are based on measurements at Potsdam. As mentioned and investigated by Wild et al. (2021), Potsdam is one of the longest and best maintained operational radiation monitoring stations, and its global radiation record can be considered representative for a substantial area in central Europe.

The fact that the increase in global radiation during the brightening phase 1980-2020 outweighs the decrease during the dimming phase 1950-1980 could be due to a trend of decreasing cloud cover during the brightening phase. However, an examination of the development of the cloud cover at Potsdam shows an approximately constant distribution in the long term (Figure 3). From 1982-2020 there is a non-significant decrease of -0.1 octas in the summer half-year and a non-significant increase of +0.5 octas in the winter half-year. This cannot have had a relevant influence on the variation of global radiation, although global radiation in individual half-years was of course modulated by the variability of cloud cover. Potsdam also shows significantly decreasing cloud cover from 1984-1994 and from 1996-2007, as shown for all of Europe by TANG et al. (2012). However, for an overall view of the last four decades, the overall trend must be considered.

The influence of aerosols seems to be the only remaining explanation of the long-term changes of global radiation (see section 1). Their radiative influence depends on their concentration, size distribution and chemical composition. A higher radiation influence means more scattering, more absorption of sunlight and therefore less direct solar radiation and more diffuse radiation. The path of direct solar radiation directly maps the path of aerosol optical depth (AOD). Both types of radiation are available for Potsdam as daily averages over the study period 1950-2020; averages for the summer and winter half-years were formed from the daily averages. The relative temporal variation of summers and summer half-years or winters and winter half-years were very similar. The results for direct solar radiation are shown in Figure 4 and Figure 5. They were classified according to the mean daily cloudiness: clear-sky (cloudiness < 2 octas), slightly cloudy (cloudiness 2-4 octas), very cloudy (cloudiness 4-6 octas), overcast (cloudiness >6 octas). For clear-sky conditions until 2017, results are in line with WILD et al. (2021).

The dimming and brightening phases are clearly formed in all four cloudiness classes. Direct solar radiation responds to changing aerosol optical parameters, even if intermittently. From 1982-2020, DSR increased by about one-third in both the summer and winter months. This increase is at least twice as large as the decrease during the dimming phase, except in the case of overcast sky, when DSR is very low and various interfering influences have a greater weight. The diffuse solar radiation has behaved in the opposite way during the two phases (i.e., less scattering led to less diffuse solar radiation during the brightening phase). However, because the decrease in diffuse radiation was less than the increase in DSR (and vice versa in the dimming phase), the result was an increase in GR overall from 1982-2020 as shown in Section 3.

The increase in DSR from 1982-2020 is consistent with other studies of aerosol radiation parameters:

MORTIER et al. (2020) explored regional time series for a set of nine optical, chemical composition and mass aerosol properties by using the observations at a set of ground-based stations. Significant decreases in aerosol optical depth (AOD) in Europe, North America, South America, North Africa and Asia were found. Modeling the aerosol trends at a global scale (including poorly measured regions and especially the oceans) led to a slight increase in global AOD of about +0.2 %/y between 2000 and 2014, primarily caused by an increase in the loads of organic aerosols, sulfate and black carbon.

A long-term trend analysis of aerosol optical properties was performed by COLLAUD COEN et al. (2020) for 52 stations situated across five continents. The time series covered at least 10 years and up to 40 years for some stations. There is evidence that scattering and backscattering coefficient trends over the last 2 decades are mostly decreasing in Europe and North America and are not statistically significant in Asia, while polar stations exhibit a mix of increasing and decreasing trends.

The studies mentioned go back as far as 1980. In Potsdam, the DSR has increased in the last 4 decades by at least twice as much as it previously decreased in the dimming phase 1950-1982. This means that the reduction in optically relevant aerosol pollution 1982-2020 would also have to be significantly larger than the increase from 1950-1982. According to "Environment Switzerland 2022", Report of the Federal Council (2023), the decrease in SO_2 emissions from

1980-2020 was actually 1.5 times the increase from 1950-1980. This relation should be representative throughout Central Europe, because the basic economic development was similar. Since the mid-19th century, coal was the most important energy source in Europe; already in 1900, SO_2 emissions were 7 times larger than in 2020 and 2/3 as large as in 1950 ("Environment Switzerland 2022"). Since sulfate reduction is the most important component of AOD reduction in Europe (e.g. COLLAUD COEN et al. (2020)), the larger increase in DSR from 1982-2020 beyond offsetting the 1950-1982 decrease is plausible in principle. Since emissions of NOx, NMVOC and NH_3 were essentially higher in 2020 than in 1950, and although aerosol mass (PM10) was still about half as high, the development of these key aerosol components does not seem to be sufficient for a doubling of the DSR increase 1982-2020 compared to the decrease in the dimming phase. Further studies are needed to understand the aerosol optical parameters back to the 1950s.

The aerosol reductions since 1982 resulting from the air pollution control measures have led to an increase in GR (in sum of DSR and diffuse radiation) of 10-19 W/m^2 on annual average (see section 3). It occurs when the sun is shining and thus shows a strong dependence on the time of day, season and weather conditions. It must be expected that it has a particularly strong influence in already radiation-rich situations, e.g. summer heat, urban heat islands, soil drying or convective processes.

Based on these results, the influence of the development of GR on surface air temperature in the period from 1950-2020 was quantitatively estimated.

5. Influence of variation of global radiation on surface air temperature

5.1 Estimation of global radiation based on sunshine duration

At the Swiss stations, measurements of global radiation (GR) extend only to 1981. Due to the close relationship between GR and sunshine duration (SSD), GR could be estimated with SSD for the periods without measurement. This relationship strongly depends on the average solar elevation angle and thus depends on the season.

Figure 6 illustrates how much GR changes with one hour more of SSD (monthly sum), averaged across all six stations (GR as monthly average. The maximum is in June, the minimum in December; the standard deviation is quite small, indicating a small influence of local conditions on the relation between GR and SSD. Therefore, there is, of course, no linear relation between GR and SSD over the whole year; but for the single months, a linear relation is evidenced by high coefficients of determination r^2 of the linear correlation between SSD (monthly sums) and GR (monthly means) per month for the period 1981-2020 (Wien 1991-2020) and all the six stations (cf. Figure 7) of around 0.9 (except for the winter months).

With the Potsdam station it can be demonstrated that the relationship between GR and SSD from 1981-2020 can be extrapolated to 1950-1980 based on calendar months. For each calendar month a linear regression between GR and SSD was formed for the period 1982-2020, and thus the GR values from 1950-1981 were estimated (GR_{calc}); for the estimation period there are also measurements at Potsdam. Good agreements were found between GR_{calc} and $GR_{measured}$ for 1950-1981 with r^2 values in the range of the correlation between GR and SSD from 1982-2020. Figure 8 depicts two examples from spring (April) and summer (July), respectively. The mean value of GR_{calc} from 1950-1981 is 2-3% higher than $GR_{measured}$ in both examples, and r^2 between GR_{calc} and $GR_{measured}$ is 0.93 in both cases.

Using this approach, GR for 1950-1981 was estimated from the SSD for the four Swiss stations and used together with the German and Austrian station for further analysis as described in section 4.2.

5.2 Methodological approach

The surface air temperature is the result of many complex processes such as increasing GHG-concentrations, changing circulations in oceans and air and others, most of them not linear with time. Looking at the measured surface air temperature in the last century, we nevertheless get the impression of an essentially linear temporal development, modulated by global dimming and brightening. Figure 9 gives the example of Basel. Therefore, the methodological approach of choice to evaluate the influence of global radiation on temperature seemed to be a multiple linear regression model based on monthly values from the period 1950-2020 with

temperature as the dependent variable and GR and time as independent variables. The complexity of the dependence of the surface air temperature on various influencing variables is not an obstacle to using a multiple linear regression model. The statistical sciences were developed for complex relationships that cannot be simply expressed with formulas. Here it is important to ensure the applicability of the model by a set of statistical standard tests. The tests for the approach in this study are described as follows:

T1: determined regression coefficient for GR is significant (error probability $p_{GR}<0.05$).

T2: Shapiro-Wilk Test for normal distribution of the residuals, i.e. the linear relation of temperature with GR as well as with time is adequate. Based on convention the test value must be >0.05.

T3: Durbin-Watson test for autocorrelation (correlation inside the dependent variables). This can be a problem especially for the correlation of time series. Since the regression is run separately for each month of the year, the problem of seasonality is eliminated. The accepted range of the Durbin-Watson test value was between 1.4 and 2.6 (for n=71 values per regression (years) and an alpha level $\alpha=0.01$).

T4: Statistical power (likelihood that a model detects an existing effect), depending on r^2 of the regression. Based on convention the statistical power must be >0.80, the maximum value is 1.

T5: Variance Inflation Factor (VIF) to measure multicollinearity of the independent variables, or of the linear combination of the independent variables in the regression. In the present model, time and GR are the independent variables. Time is per se independent if relativistic effects are irrelevant. But GR could be dependent on time (structural multicollinearity) or the effect of GR on temperature could be dependent on time (sample-based multicollinearity). The VIF is calculated regarding both types of multicollinearity. A value of 1 means no multicollinearity; VIF values above 4 suggest possible multicollinearity; values above 10 indicate serious multicollinearity.

The model was run for each calendar month of the year and each station. A regression result was only used to determine the influence of global radiation on surface air temperature if all

five tests were fulfilled, i.e. if at least one test failed, the contribution of that month to the temperature influence of GR was set to zero.

For GR, the regression period 1950-2020 includes the phase of global brightening and global dimming. The coefficient expressing the influence of GR on temperature is derived for the whole period.

5.3 Results

In total 72 multiple linear regressions were performed: 12 months each at six stations. For the summer half year (April to September), 3 of 36 regressions did not fulfil all the five tests (s. section 4.2), for October and March 3 of 12 regressions failed, and in winter (November to February), 21 of 24 regressions did not fulfil all the tests (cf. Table 2). More irradiation during the day often means more outgoing longwave radiation in the entire day. In wintertime, this may lead to lower temperatures depending on the exposure of the measurement site to ground-level atmospheric inversions. The temperature effect in winter can vary much more than in the summer half-year.

The three rejected regressions in the summer half-year were due to failed Shapiro-Wilk tests (linearity); the rejected regressions in the winter half-year (October to March) all had error probabilities (p) of the GR coefficient above the threshold of significance, partly with failed tests concerning Shapiro-Wilk and statistical power. The tests of Durbin-Watson (autocorrelation) and VIF (variance inflation factor; multicollinearity between the independent variables) were all satisfied.

For the successful regressions, the statistical power (conventionally should be >0.80, the maximum value is 1), the test values were between 0.90 and 1.00 with an average of 0.99; the test values for VIF (A value of 1 means no multicollinearity; VIF values above 4 suggest possible, above 10 indicate serious multicollinearity) were between 1.00 and 1.18 with an average of 1.04. The error probabilities ($p < 0.05$) of the successful regressions had a maximum of $9*10^{-5}$ in the summer half-year and of 0.029 in the winter half-year.

Thus, most regressions fulfilled the tests and led to significant results. The results of months with at least one unfulfilled test were not included in the calculation of the effects of global radiation on temperature.

The regression coefficients for each month were summarized across all six stations to mean values with standard deviation. The GR coefficient concerns the change of temperature (monthly mean) per unit (W/m^2) of global radiation (monthly mean) (Figure 10). In the summer half-year this coefficient is +0.04 to +0.06 °C/(W/m^2) with a quite small standard deviation. The change of temperature with global radiation in the monthly mean hardly seems to depend on location. In March and October the scatter is already larger and in winter too few significant results were available.

The other coefficient in the regression concerns the continuous increase of temperature with time from 1950-2020. The time dependence of the monthly mean temperature varies on average across all six stations between +0.016 and +0.036 °C/year (Figure 11). This corresponds to an increase of +1.7 °C in Central Europe in the summer half-year from 1950 to 2020 regardless of the effect of fluctuating global radiation. No corresponding statement can be made for the winter half-year, and thus also not for the entire year. Here, the standard deviation per month across all six stations is larger, because local and regional effects play a larger role.

September is the month with the lowest temperature increase, August and October have the highest. Similar strong differentiations between the months were also found in a study on climate change in southeastern Switzerland (THUDIUM and CHÉLALA, 2020).

From the determined dependence of temperature on global radiation, the temperature effect of global dimming and brightening could be calculated for each station. This effect was derived for each calendar month with reference to the average of global radiation from 1950-2020, and the trend of this effect in the dimming and in the brightening phase was determined, and further summarized for the summer half year and the entire year, respectively.

For the three stations with one failed month in the regressions for the summer half-year, the averages for the summer half-year were formed by the other five months. For the winter half-year, too many months failed for that procedure, so these months contributed with zero to the

calculated temperature effects of global radiation, thus the calculations for the entire year show the minimum effects.

The temperature changes due to fluctuating global radiation are shown in Figure 12 (left side) for the summer half-year and the entire year for all six stations: cooling during the global dimming phase, warming during the global brightening phase and the sum of both phases, i.e. the temperature increase from 1950-2020 due to the overall increase in global radiation over the whole period.

On average across all six stations, in the summer half-year global dimming led to a relative cooling of -0.6 °C and global brightening to a warming of +1.1 °C. Over the entire period 1950-2020, the overall increase in global radiation resulted in a warming of +0.5 °C, in consequence of the overall increase of global radiation in that period (cf. Chapter 3). For the entire year, the corresponding values are -0.3 °C during global dimming period, +0.6 °C during global brightening period and over the entire period 1950-2020 +0.3 °C due to the influence of global radiation on temperature.

These findings are to be compared directly with the measurements of temperature (cf. Figure 12, right side, for the entire period 1950-2020). **For the summer half-year**, the mean influence of the variable time on temperature, representing the long-term continuous temperature increase, can also be derived across all six stations. Thus, the total temperature development calculated from the results of linear regressions can be directly compared to the temperature measurements for the summer half-year. Based on the average of the six stations, the measurements give a temperature development for the dimming period of just 0.0 °C (regression model +0.1 °C), for the brightening period +2.1 °C (regression model +2.0 °C), and over the whole period 1950-2020 +2.13 °C (regression model +2.16 °C). The scattering at the single stations is larger. Overall, the model results are reasonable in view of the comparison with the measurements. In combination with the section above, the fraction attributable to global radiation change within the total temperature increase for the summer half-year is about a quarter (+0.5 °C) in the entire period 1950-2020, and about half (+1.1 °C) for the brightening period.

For the entire year, based on the average of the six stations, the measurements give a temperature development for the dimming period nearly +0.3 °C, for the brightening period nearly +1.9 °C, over the whole period 1950-2020 +2.13 °C. The influence of the variable time

on temperature cannot be derived for the entire year, only for October to March, because there are too few successful regressions for November to February. The results of the influence of global radiation on temperature are mainly based on these 8 months outside the winter, and therefore show minimum effects, The fraction attributable to global radiation change within the total temperature increase for the entire year is about 14% (+0.3 °C) for the entire period 1950-2020, and about one third (+0.6 °C) for the brightening period.

6. Conclusions

The overall temperature increase from 1950-2020 is dominated by a temporally continuous temperature increase (global warming). However, a fraction of this increase (+0.3 °C for the entire year resp. +0.5 °C for the summer half-year) is attributed to the increase of global radiation in the brightening period, exceeding the decrease in the dimming period.

Regarding the brightening period in the last four decades (ca. 1980-2020), the fraction of the increase of global radiation within the total temperature increase is substantial, amounting to about one third for the entire year (about +0.6 °C), and even half for the summer half-year (about +1.1 °C).

Fluctuating global radiation has turned out to stem mainly from varying aerosol loads and to have a clear impact on the evolution of surface air temperature over the past seven decades in Central Europe. Just as increasing air pollution was mainly responsible for the period of global dimming, the period of brightening was in large part a consequence of successful air pollution abatement, especially with regard to sulfates. Similar investigations on global radiation for other regions in the world could be helpful.

Acknowledgments

We appreciate the support of MeteoSchweiz and ZAMG in the field of global radiation measurements. Special thanks to Mike Chudacoff for editing the English text.

Statements & Declarations

Competing Interests

The authors have no relevant financial or non-financial interests to disclose.

Author Contributions

The study conception and design were set up by Jürg Thudium. Data collection and presentation were performed by Carine Chélala. Analysis was performed by all authors. The first draft of the manuscript was written by Jürg Thudium and both authors commented on previous versions of the manuscript. Both authors read and approved the final manuscript.

Data Availability

The datasets (monthly values) analyzed during the current study are available as follows: Switzerland: Homogenized data of temperature are available by https://www.meteoschweiz.admin.ch/home/klima/schweizer-klima-im-detail/homogene-messreihen-ab-1864.html. Homogenized data of sunshine duration and global radiation have to be purchased by https://www.meteoschweiz.admin.ch/home/service-und-publikationen/produkte.subpage.html/de/data/products/2014/bodenstationsdaten.html or may be available from the authors upon reasonable request if permitted by MeteoSchweiz.

Austria: Homogenized data of temperature and sunshine duration are available by http://www.zamg.ac.at/histalp/dataset/station/csv.php. Data of global radiation have to be purchased by https://www.zamg.ac.at/cms/de/klima/produkte-und-services/daten-und-statistiken/messdaten or may be available from the authors upon reasonable request if permitted by ZAMG.

Germany: Homogenized data of temperature, sunshine duration and global radiation are available by https://opendata.dwd.de/climate_environment/CDC/.

Code Availability

The code for the statistical model may be available confidentially from the authors upon reasonable request.

Consent for publication

Both authors and their affiliation consent for publication of this manuscript.

Ethics approval

No humans or animals were involved in this study.

References

AAS, WENCHE, AUGUSTIN MORTIER, VAN BOWERSOX, RIBU CHERIAN, GREG FALUVEGI, HILDE FAGERLI, JENNY HAND, ZBIGNIEW KLIMONT, CORINNE GALY-LACAUX, CHRISTOPHER M. B. LEHMANN, CATHRINE LUND MYHRE, GUNNAR MYHRE, DIRK OLIVIÉ, KEIICHI SATO, JOHANNES QUAAS, P. S. P. RAO, MICHAEL SCHULZ, DREW SHINDELL, RAGNHILD B. SKEIE, ARIEL STEIN, TOSHIHIKO TAKEMURA, SVETLANA TSYRO, ROBERT VET, XIAOBIN XU, 2019: Global and regional trends of atmospheric sulfur. Sci Rep **9**, 953, DOI: 10.1038/s41598-018-37304-0.

AUER, I., R. BÖHM, A. JURKOVIC, W. LIPA, A. ORLIK, R. POTZMANN, W. SCHÖNER, M. UNGERSBÖCK, C. MATULLA, K. BRIFFA, PD. JONES, D. EFTHYMIADIS, M. BRUNETTI, T. NANNI, M. MAUGERI, L. MERCALLI, O. MESTRE, J-M. MOISSELIN, M. BEGERT, G. MÜLLER-WESTERMEIER, V. KVETON, O. BOCHNICEK, P. STASTNY, M. LAPIN, S. SZALAI, T. SZENTIMREY, T. CEGNAR, M. DOLINAR, M. GAJIC-CAPKA, K. ZANINOVIC, Z. MAJSTOROVIC, E. NIEPLOVA, 2007: HISTALP – Historical instrumental climatological surface time series of the greater Alpine region 1760-2003. International Journal of Climatology **27**, 17-46, DOI: 10.1002/joc.1377.

BEGERT, M., G. SEIZ, T. SCHLEGEL, M. MUSA, G. BAUDRAZ, M. MOESCH, 2003: Homogenisierung von Klimamessreihen der Schweiz und Bestimmung der Normwerte 1961-1990. MeteoSchweiz, Schlussbericht des Projektes NORM90, 170p

BOÉ, J., 2016: Modulation of the summer hydrological cycle evolution over western Europe by anthropogenic aerosols and soil-atmosphere interactions, Geophys. Res. Lett. **43**, 7678–7685, DOI:10.1002/2016GL069394.

BÖHM, R., I. AUER, W. SCHÖNER, M. GANEKIND, C. GRUBER, A. JURKOVIC, A. ORLIK, M. UNGERSBÖCK, 2009: Eine neue Webseite mit instrumentellen Qualitäts-Klimadaten für den Grossraum Alpen zurück bis 1760. Wiener Mitteilungen **216.** Hochwässer: Bemessung, Risikoanalyse und Vorhersage

CHARLSON, R.J., S.E. SCHWARTZ, J.M. HALES, R.D. CESS, J.A. OAKLEYJR, J.E. HANSEN, D.J. HOFMAN, 1992: Climate Forcing by Anthropogenic Aerosols. Science 255: 423 – 430

COLLAUD COEN, MARTINE, 2020: Multidecadal trend analysis of in situ aerosol radiative properties around the world. Atmos. Chem. Phys., 20, 8867–8908, 2020. https://doi.org/10.5194/acp-20-8867-2020

DÜRR, B., D. SCHUMACHER, M. BEGERT, D. VAN GEIJTENBEEK, 2016: Globalstrahlungsmessung im A-NETZ – Update der Bearbeitung bis zum SMN-Übergang. Fachbericht MeteoSchweiz 262, 30 p

FEDERAL COUNCIL OF SWITZERLAND, 2023: Report 'Environment Switzerland 2022'. https://www.bafu.admin.ch/bafu/en/home/documentation/reports/environmental-report.html.

FEDERAL OFFICE FOR THE ENVIRONMENT (FOEN), 2020: Luftqualität 2019. Messresultate des Nationalen Beobachtungsnetzes für Luftfremdstoffe (NABEL). Bundesamt für Umwelt, Bern. Umwelt-Zustand Nr. **2020,** 28 p.

FOUKAL, P., C. FRÖHLICH, H. SPRUIT, T. M. L. WIGLEY, 2006: Variations in solar luminosity and their effect on the Earth's climate, Nature **443**, 161– 166.

KIEHL, J.T., B.P. BRIEGLEB, 1993: The Relative Roles of Sulfate Aerosols and GreenhouseGases in Climate Forcing. Science 260: 311-314

KUHN, M., M. OLEFS, 2020: Elevation-Dependent Climate Change in the European Alps. Oxford Research Encyclopedia of Climate Science, DOI: 10.1093/acrefore/9780190228620.013.762.

LIEPERT, B. G., 2002: Observed reductions of surface solar radiation at sites in the United States and worldwide from 1961 to 1990, Geophys. Res. Lett., 29(10), 1421, DOI:10.1029/2002GL014910.

MOESCH, M., A. ZELENKA, 2004: Globalstrahlungsmessung 1981-2000 im ANETZ. MeteoSchweiz, Arbeitsbericht 207

MORTIER, AUGUSTIN et al., 2020: Evaluation of climate model aerosol trends with ground-based observations over the last 2 decades – an AeroCom and CMIP6 analysis. Atmos. Chem. Phys., 20, 13355–13378, 2020. https://doi.org/10.5194/acp-20-13355-2020.

NORRIS, J. R., M. WILD, 2007: Trends in aerosol radiative effects overEurope inferred from observed cloud cover, solar ''dimming'' and solar ''brightening'', J. Geophys. Res. **112**, D08214, DOI:10.1029/2006JD007794.

OHMURA, A., H. LANG, 1989: Secular variation of global radiation in Europe, in IRS '88: Current Problems in Atmospheric Radiation, edited by J. Lenoble and J. Geleyn, pp. 298– 301, Deepak, Hampton, Va.

OHMURA, A., 2006: Observed long-term variations of solar irradiance at the Earth's surface, Space Sci. Rev., 125, 111 –128, DOI:10.1007/s11214-006-9050-9.

RUCKSTUHL, C., R. PHILIPONA, K. BEHRENS, M. C. COEN, B. DÜRR, A. HEIMO, C. MÄTZLER, S. NYEKI, A. OHMURA, L. VUILLEUMIER, M. WELLER, C. WEHRLI, A. ZELENKA, 2008: Aerosol and cloud effects on solar brightening and the recent rapid warming. Geophysical Research Letters, 35, L12708, DOI: 10.1029/2008GL034228.

SCHERRER, S. C., M. BEGERT, 2019: Effects of large-scale atmospheric flow and sunshine duration on the evolution of minimum and maximum temperature in Switzerland. Theoretical and Applied Climatology **138**, 227–235, DOI: 10.1007/s00704-019-02823-x.

STANHILL, G., S. COHEN (2001), Global dimming: A review of the evidence for a widespread and significant reduction in global radiation with discussion of its probable causes and possible agricultural consequences, Agric. For. Meteorol. **107**, 255– 278.

TANG, Q. et al., 2012: European Hot Summers Associated with a Reduction of Cloudiness. J. Climate **25**, 3637–3644, DOI:10.1175/JCLI-D-12-00040.1.

THUDIUM, J., C. CHÉLALA, 2020: Jber. Natf. Ges. Graubünden **121**, p 47 – 62. [peer-reviewed annual journal of the natural research society of Grisons, Switzerland]

Wild, M., et al. (2005), From dimming to brightening: Decadal changes in solar radiation at Earth's surface, Science **308**, 847– 850.

WILD, M., S. WACKER, S. YANG, A. SANCHEZ-LORENZO, 2021: Evidence for clear-sky dimming and brightening in central Europe. Geophysical Research Letters **48**, e2020GL092216, DOI: 10.1029/2020GL092216.

Figures and tables

Table 1: Names and coordinates of the measuring stations used in this study. SSD: Sunshine duration; GR: Global radiation.

Name of station	Abbr.	Longitude	Latitude	Altitude	Data availability for this study since		
		[deg]	[deg]	[m a.s.l.]	SSD	Temp.	GR
Basel / Binningen	BAS	7.583	47.533	316	1950	1950	1981
Bern / Zollikofen	BER	7.467	46.983	553	1950	1950	1981
Genève / Cointrin	GVE	6.128	46.248	411	1950	1950	1981
Zürich / Fluntern	ZRH	8.567	47.383	556	1950	1950	1981
Potsdam	POT	13.060	52.380	81	1950	1950	1950
Wien Hohe Warte	WIE	16.356	48.249	198	1950	1950	1951

Figure 1: Map with the analyzed measuring stations in Austria, Germany and Switzerland. For more information on the stations see Table 1.

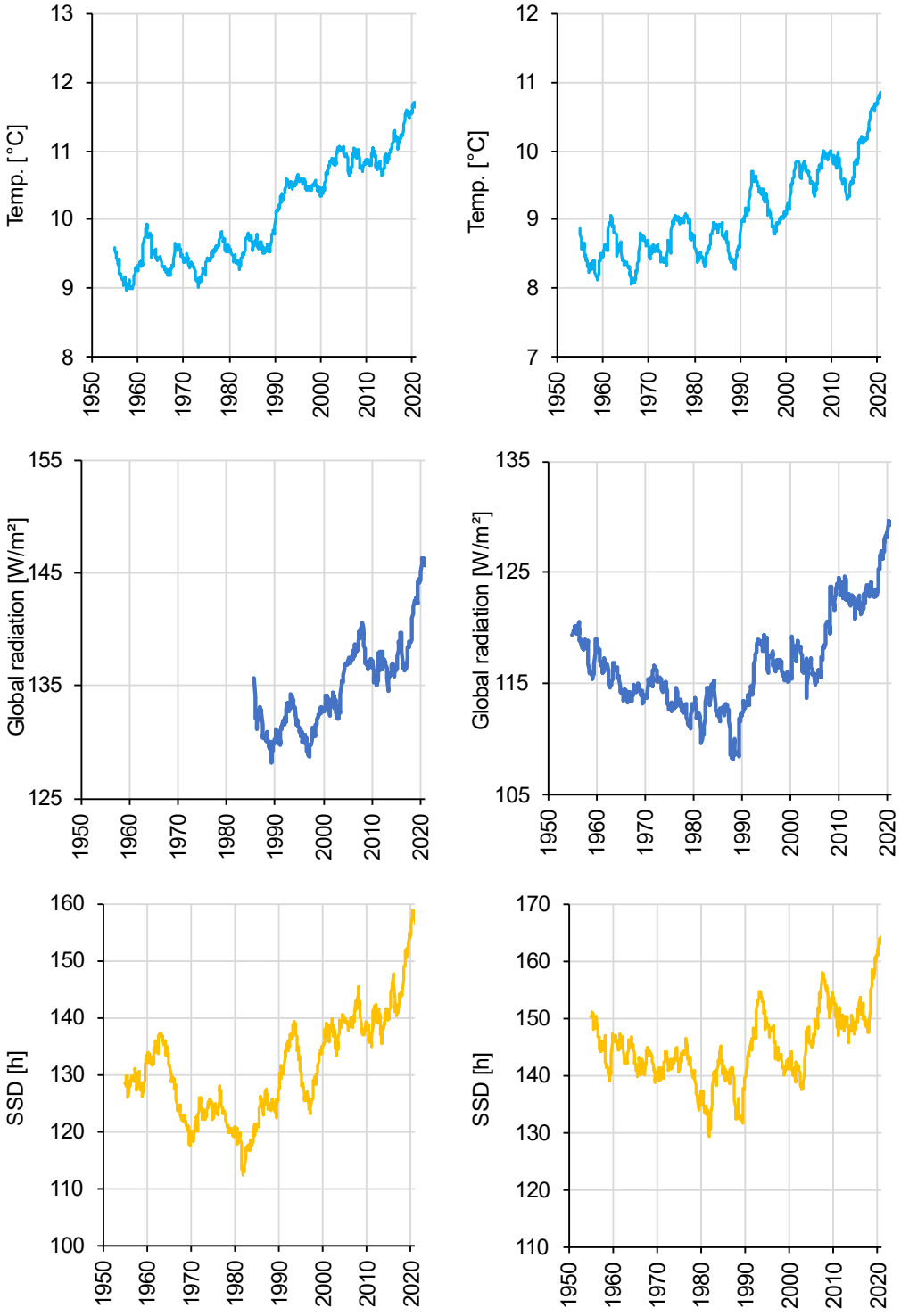

Figure 2: Temperature (top), global radiation (GR; middle) and sunshine duration (SSD; bottom) at Basel (left) and Potsdam (right), gliding 5-years-averages, 1950-2020. For all stations, the range of values includes 5 °C for the temperature, 30 W/m² for global radiation and 60 h for the SSD, respectively.

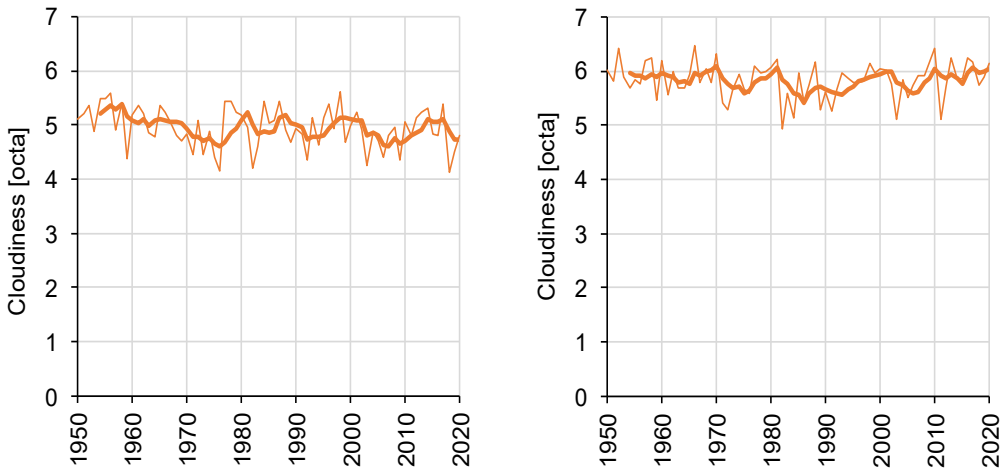

Figure 3: Mean Cloudiness at Potsdam for the summer- (left) resp. winter half years (right), annual values (thin lines) and gliding 5-years-averages (thick lines), 1950-2020.

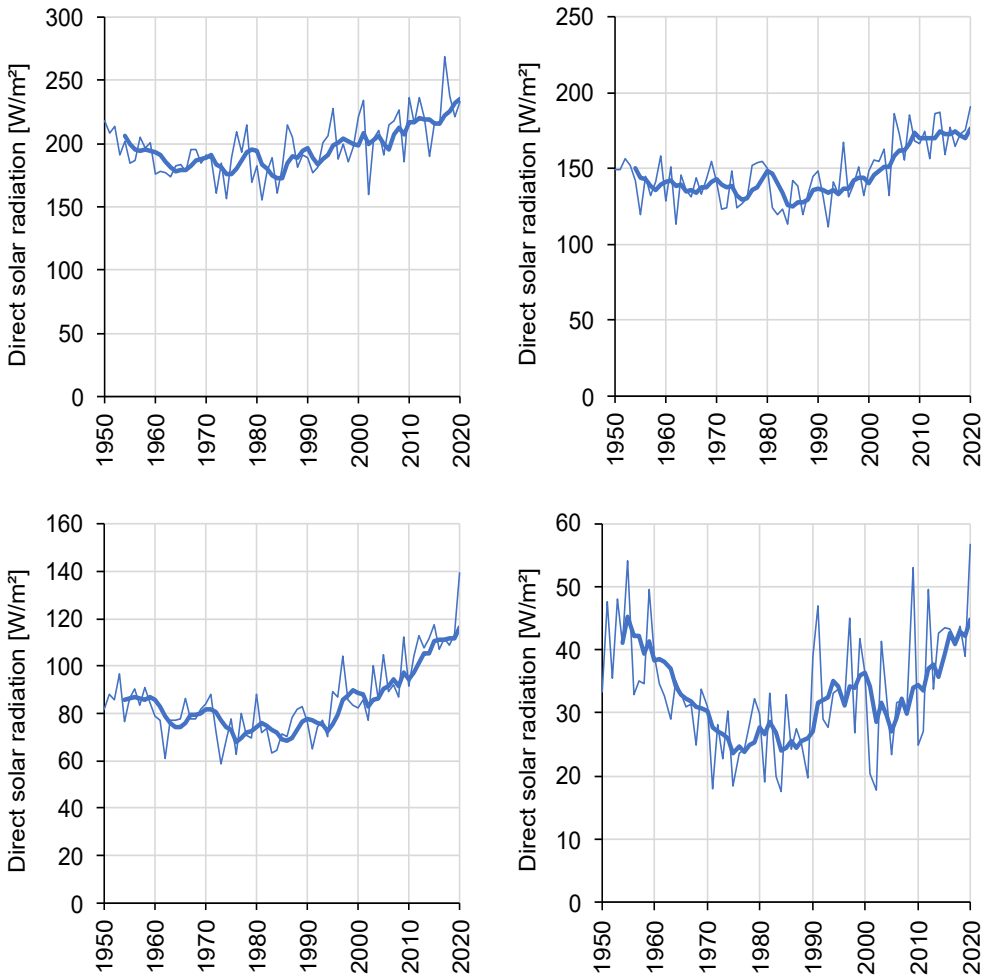

Figure 4: Direct solar radiation /DSR) at Potsdam, 1950-2020, **summer** half years, for cloudiness < 2 octas (top left), cloudiness 2-4 octas (top right), cloudiness 4-6 octas (bottom left) and cloudiness >6 octas (bottom right).

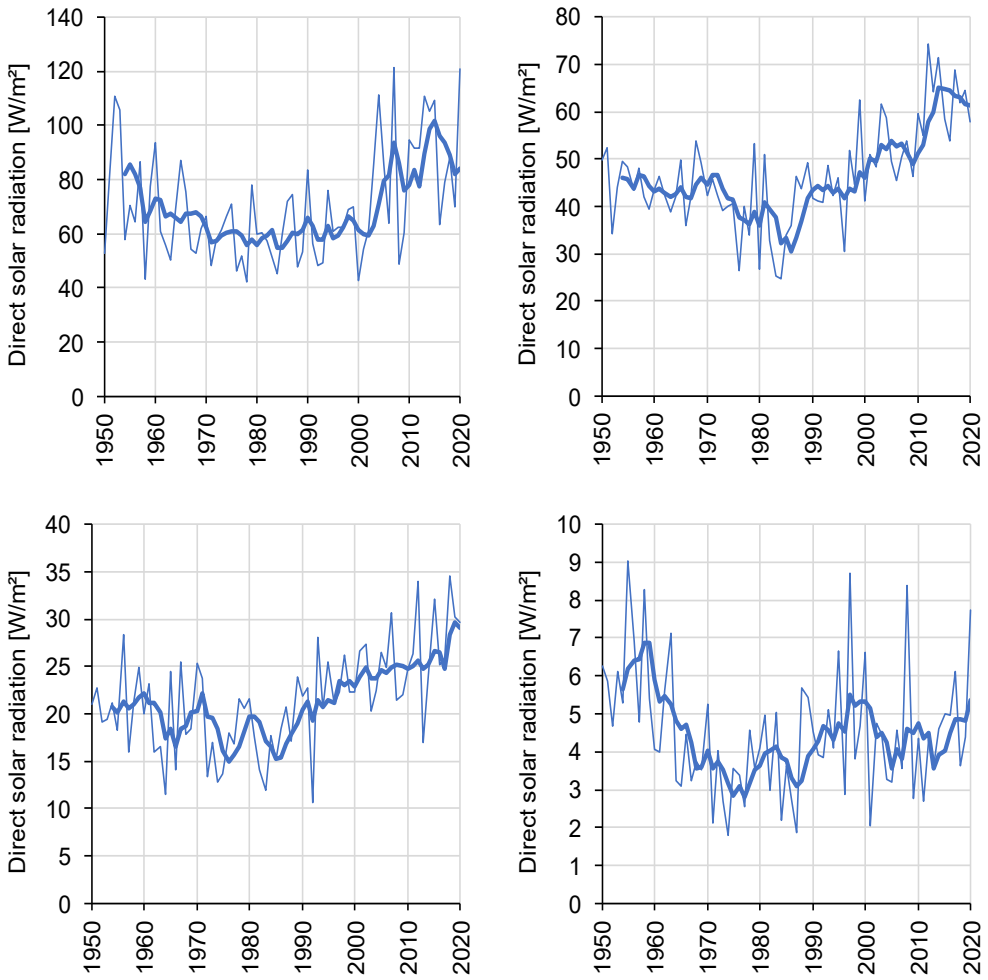

Figure 5: Direct solar radiation (DSR) at Potsdam, 1950-2020, **winter** half years, for cloudiness < 2 octas (top left), cloudiness 2-4 octas (top right), cloudiness 4-6 octas (bottom left) and cloudiness >6 octas (bottom right).

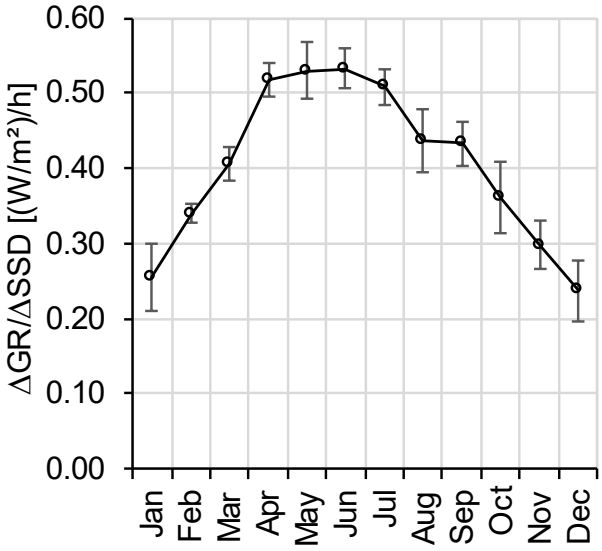

Figure 6: Change of monthly mean global radiation (GR) per hour of monthly sum of sunshine duration (SSD), calculated from linear regression between GR and SSD for each month and each station from 1981-2020 (Wien 1991-2020). Average is across all stations used in this study. The black bars show the standard deviation.

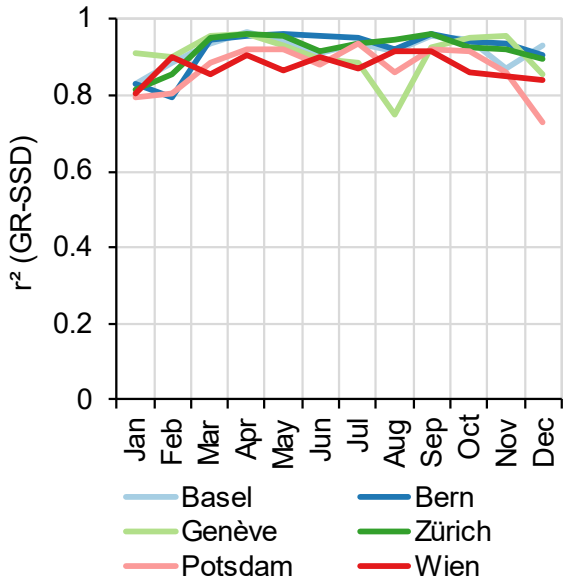

Figure 7: Coefficient of determination r^2 of the correlation between sunshine duration (SSD; monthly sums) and global radiation (GR; monthly means) per month, for the six stations), 1981-2020 (Wien 1991-2020).

Table 2: Success of all five statistical tests or failure of at least one test (X) per station and month.

	Jan	Feb	Mar	Apr	May	Jun	Jul	Aug	Sep	Oct	Nov	Dec
BAS	X	X	✓	✓	✓	X	✓	✓	✓	✓	X	X
BER	X	X	✓	✓	✓	✓	✓	✓	✓	✓	X	X
GVE	X	X	✓	✓	✓	✓	X	✓	✓	✓	X	X
ZRH	X	X	✓	✓	✓	✓	✓	✓	✓	✓	✓	X
POT	✓	✓	X	✓	X	✓	✓	✓	✓	X	X	X
WIE	X	X	✓	✓	✓	✓	✓	✓	✓	X	X	X

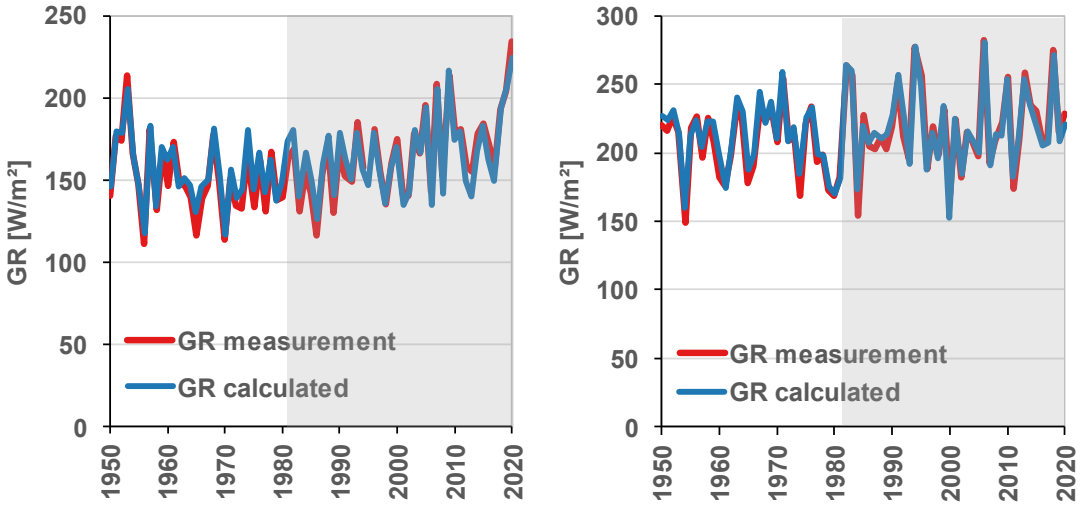

Figure 8: Variation of measured ($GR_{measured}$) and calculated (GR_{calc}) global radiation at Potsdam for April (left) and July (right) 1950-2020. GR_{calc} was determined from a linear regression with $GR_{measured}$ and SSD from 1982-2020 (time range highlighted in blue).

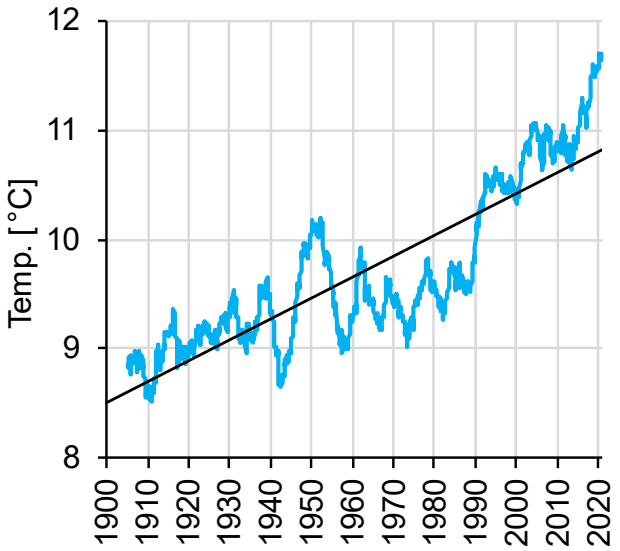

Figure 9: Variation of measured temperature at Basel, gliding 5-years-averages, 1900-2020, with trendline.

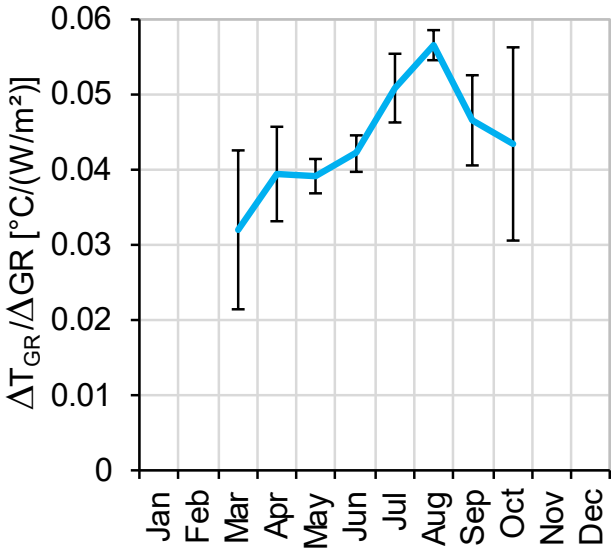

Figure 10: Change of monthly mean temperature per unit (W/m²) of monthly mean global radiation (GR). Result of linear regression of monthly mean temperature (dependent variable) with time and monthly mean global radiation (independent variables), 1950-2020, per month. Mean values over all six stations with standard deviation (black bars) for each month. Illustrative example: In July, an increase of the mean global radiation by 1 W/m² results in an increase of the monthly mean temperature by 0.05 °C.

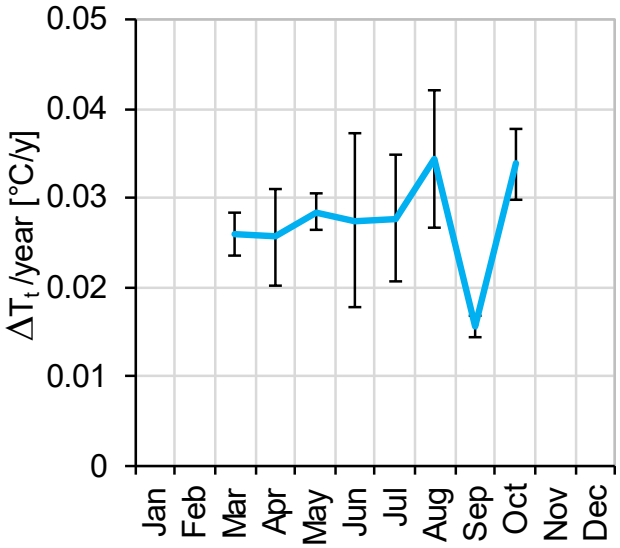

Figure 11: Change of monthly mean temperature per year. Result of linear regression of monthly mean temperature (dependent variable) with time and monthly mean global radiation (independent variables), 1950-2020, per month. Mean values across all six stations with standard deviation (black bars) for each month. Illustrative example: In July, there is a linear increase of the monthly mean temperature by 0.028 °C per year.

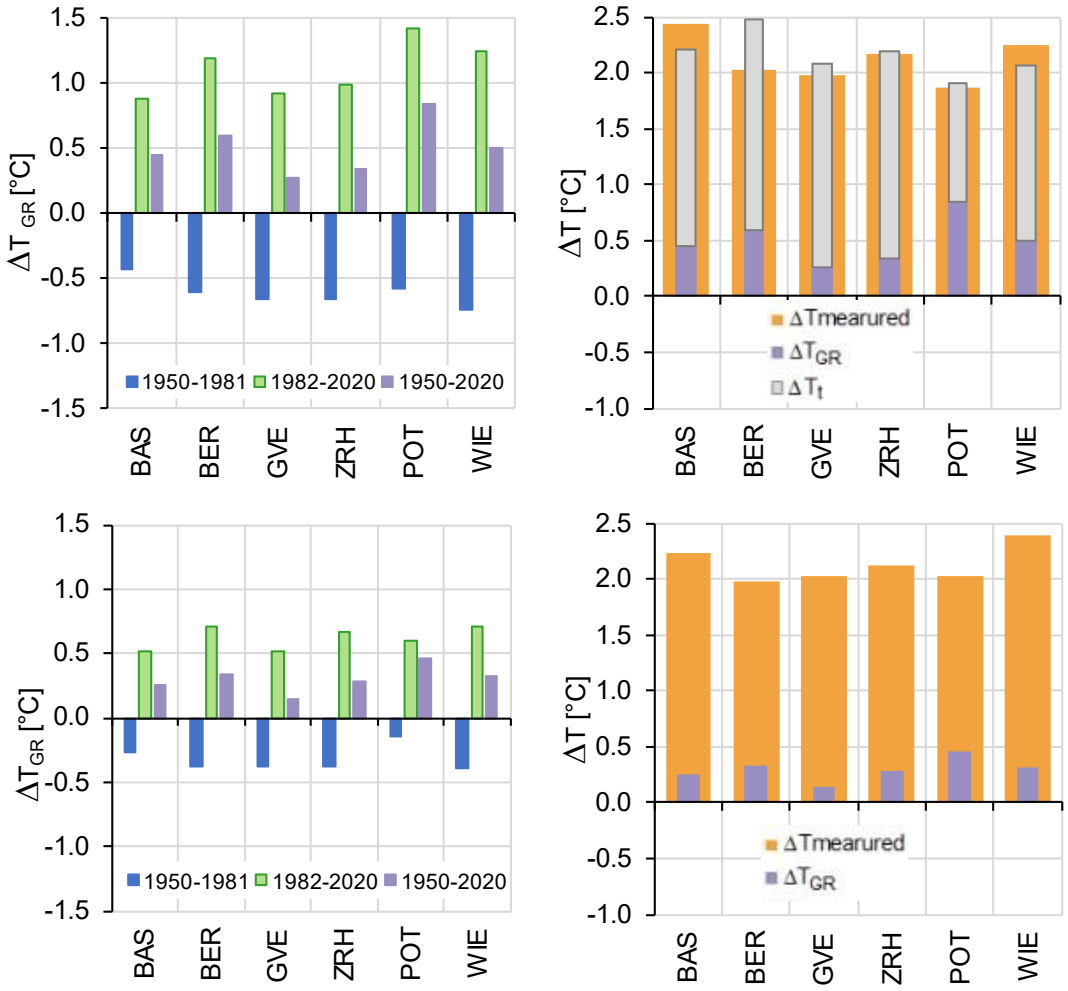

Figure 12: Left side: Change of mean temperature of summer half-year (April-September; top) and year (bottom) per period from1950-1981, 1982-2020 and 1950-2020 respectively. Result of linear regression of monthly mean temperature with time and monthly mean global radiation, 1950-2020. Values for all six stations. Illustrative Example: At ZRH (Zurich) for the summer half-year there was a temperature decrease from 1950-1981 due to decrease of global radiation (dimming) of -0.65 °C. From 1982-2020 there was a temperature increase due to an increase in global radiation (brightening) of +1.0 °C. For the whole period from 1950-2020 the temperature increased by +0.35 °C due to the total resulting increase of global radiation.

Right side: Change of mean temperature of summer half-year (April-September; top) and year (bottom) or the period 1950-2020. ΔT_{GR} respectively ΔT_t: Results of linear regression of

monthly mean temperature with time and monthly mean global radiation; influence of global radiation (ΔT_{GR}) respectively of time (ΔT_t). No influence of time can be derived for the entire year. $\Delta T_{measured}$: Change of mean temperature of summer half-year (April-September; top) and year (bottom) over the period 1950-2020, directly derived from measurements.